A Numerical Study on THZ-Wave Generation and Detection of Metal-Oxide-Semiconductor Field-effect Transistor

Cheng Wang, Xuehao Mou, Jin He, Yun Ye, Hongyu He, and Yu Cao

Peking University Shenzhen SOC Key Laboratory, PKU-HKUST Shenzhen-Hongkong Institution, Shenzhen 518057, P.R.China

ABSTRACT

A numerical method is developed in this paper to simulate FET-based THz wave generation and detection. The method is derived directly from the hydrodynamic equations and implemented in Matlab coding. Simulation results are compared with the previous theory, proving the validity of the developed numerical method and providing useful data for MOS field effect transistor THZ generation and detection analysis and optimization.

Keywords:THz-wave, FET, Hydrodynamic Equation, Numerical Simulation

I. Introduction

Terahertz (THz) technologies have been paid much attention in recent years due to its potential application in remote sensing, biomedical, and space communication. Compared with other methods, THz generation and detection based on the 2-dimensional electron gas (2DEG) in field-effect transistors (FET) have exhibited lots of advantages such as frequency tunable, extremely compact and room temperature workable. In 1977, Allen et al demonstrated that the infrared radiation is absorbed by the silicon MOSFET from experiments. Later, Tsui reported weak infrared radiation from the inversion layers in the silicon based FET [1].

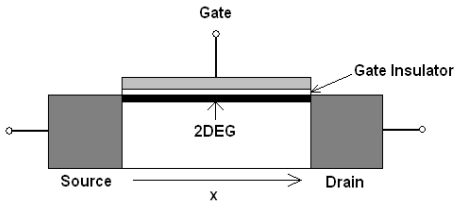

Fig. 1 2DEG in an FET

Paralleling the advance of the experimental study, many theories for THz generation and detection have also been developed by Dyakonov, Shur, Ryzhii, Dmitriev, Furman [2-7]. The theories are all based on the basic hydrodynamic equations (continuiry equation and Euler equation) derived by Dyakonov and Shur [6]. Yet the equations are theoretically solved by small signal approximation, while accurate solutions are needed for the improvement of the theories. Therefore, a numerical simulation method is needed to verify the developed theories, and optimize the THz device structure and design. However, the numerical simulation methods and tools for THz FET have not been available in the public domain and commercial EDA business.

In this paper, a new numerical method to simulate the THz FET is developed and tested. In this method the variables and coefficients used are more directly derived from the original hydrodynamic equations, which have clearer physical meanings for the device characteristics analysis and structure optimization, hence this method is of great help for designers.

The details of the method are introduced in Section II. Two representative theories are simulated and discussed in Section III and IV: the instability method of THz generation [2] and the resonant detection of THz signals [4]. Discussion is in Section V and conclusion is drawn in Section VI.

II. The Numerical Method

The hydrodynamic equations are as below [2]:

$$\frac{\partial U}{\partial t}+\frac{\partial (Uv)}{\partial x}=0 \qquad (1)$$

$$\frac{\partial v}{\partial t}+v\frac{\partial v}{\partial x}=-\frac{e}{m}\frac{\partial U}{\partial x}-\frac{v}{\tau_m}+\frac{K}{U}\frac{\partial^2 v}{\partial x^2} \qquad (2)$$

In the equations, U is the gate-to-channel voltage, v is the local electron velocity, τ_m describes the momentum relax time and K is determined by the viscosity of the 2DEG. One can choose K=0 or not to decide the method is used for THz detection or generation [2, 4]. The boundary and initial conditions are also different for THz generation and detection.

Define $u=U/U_0$, $v=v/s$, $\eta=x/L$, $\tau=ts/L$, $\tau_m'=\tau_m s/L$, $\kappa=K/LsU_0$. Here L is the length of the channel. x=0 denotes the source contact and x=L the drain contact. One obtains the dimensionless equations:

$$\frac{\partial u}{\partial \tau}+\frac{\partial (uv)}{\partial \eta}=0 \qquad (3)$$

$$\frac{\partial (uv)}{\partial \tau}+\frac{\partial}{\partial \eta}(uv^2+\frac{u^2}{2})+\frac{uv}{\tau_m'}=\kappa\frac{\partial^2 v}{\partial \eta^2} \qquad (4)$$

To simulate the THz wave during the dimensionless time interval [0, T], define $\Delta\tau=T/M$, $\Delta\eta=1/N$, and F_i^j as the value of function F at $\eta_i=i\Delta\eta$, $\tau_j=j\Delta\tau$ to construct the mesh grids.

Vectors below are defined:

$$q_k^n=\begin{bmatrix} u_k^n \\ (uv)_k^n \end{bmatrix} \quad F_k^n=\begin{bmatrix} (uv)_k^n \\ (uv^2+u^2/2)_k^n \end{bmatrix}$$

$$G_k^n=\begin{bmatrix} 0 \\ (uv/\tau_m')_k^n \end{bmatrix} \quad H_k^n=\begin{bmatrix} 0 \\ \kappa(v_{k+1}^n-2v_k^n+v_{k-1}^n)/(\Delta\eta)^2 \end{bmatrix}$$

Define L_η as the spatial central-difference operator in the space, Δ_τ the temporal forward-difference operator. One then obtains the difference version of (3)(4):

$$\Delta_\tau q_k^n + L_\eta F_k^{n+1} + G_k^n = H_k^n \quad (5)$$

Taylor expansion is applied:

$$F_k^{n+1} \approx F_k^n + A_k^n (q_k^{n+1} - q_k^n) \quad (6)$$

$$A_k^n = \begin{bmatrix} \partial F_1/\partial q_1 & \partial F_1/\partial q_2 \\ \partial F_2/\partial q_1 & \partial F_2/\partial q_2 \end{bmatrix}_k^n = \begin{bmatrix} 0 & 1 \\ u - v^2 & 2v \end{bmatrix}_k^n$$

Applying (6) to (5), one obtains:

$$q_k^{n+1} + TA_{k+1}^n q_{k+1}^{n+1} - TA_{k-1}^n q_{k-1}^{n+1} = q_k^n - TF_{k+1}^n + TF_{k-1}^n + TA_{k+1}^n q_{k+1}^n - TA_{k-1}^n q_{k-1}^n - G_k^n + H_k^n \quad (7)$$

Here $T=\Delta\tau/2\Delta\eta$. Boundary conditions are then added to the equations. Usually the gate-to-source voltage and the drain current are given to determine the THz-wave in the FET, which is valid in both THz generation and detection. That is to say, u(0) and uv(1) are given. Because of the existence of $\partial^2 v/\partial\eta^2$, another boundary equation is needed. After examining the side contact of the channel, one can choose $v_\eta(0)=0$ which denotes $\partial^2 v/\partial\eta^2 = (v_n^1 - v_n^0)/(\Delta\eta)^2$. Hence, at η=0. $v_n^0 = v_n^{-1}$

At η=0, use equation (3) to describe boundary condition:

$$\frac{(uv)_0^{n+1} - (uv)_0^n}{\Delta\tau} + \frac{(F_2)_1^n - (F_2)_0^n}{\Delta\eta} + \left(\frac{uv}{\tau_m'}\right)_0^n = \kappa \frac{v_1^n - v_0^n}{(\Delta\eta)^2} \quad (8)$$

Similarly, at η=1 use equation (6) to describe boundary condition:

$$\frac{u_M^{n+1} - u_M^n}{\Delta\tau} + \frac{(uv)_M^n - (uv)_{M-1}^n}{\Delta\eta} = 0 \quad (9)$$

The Matlab coding is based on equations (7)(8)(9).

III. Simulation of THz Generation by instability

In reference [2], Dmitriev and Furman introduced a theory of THz generation based on the instability properties of the 2DEG. Invariant gate-to-source voltage and drain current are imposed on the FET as boundary conditions. Small-signal approximation predicts that the AC voltage and current along the channel has the form exp(-iωt), and the frequency ω has the form ω=ω'+iω'', which indicates that the oscillation has the frequency ω' and increment ω'' as below (N=1, 2, 3…):

$$\omega_n' = \frac{\pi}{2}(2N-1) \quad (10)$$

$$\omega_n'' = \frac{V_0}{s} - \frac{1}{2\tau_m'} - \frac{\kappa\pi^2}{8}(2N-1)^2 \quad (11)$$

That the increment ω_n'' decreases as N increases indicates that if $\omega_1''<0$, all modes will be damped out. When $\omega_n''>0$, all the modes ω_k'' with $k\le n$ are amplified, then the nonlinear properties are then contribute to the stabilization of the oscillation and the amplitude is proportional to certain powers of ω_1''. When $\omega_1''>>\kappa$, the case of shock wave is possible to happen, which predicts a step-like voltage and current distribution along the channel [2].

Different v_0, κ, τ_m' are chosen to simulate the conditions that the THz radiation is damped out, approximately stable, and amplified. Boundary conditions are that u(0)=1 and $v_0=V_0/s=uv(1)/u(0)=$const. Initial conditions are given as u=1, uv=0 along the channel, indicating that no current is distributed along the channel at the beginning and the voltage distribution is even. The results are shown in Fig. 2.

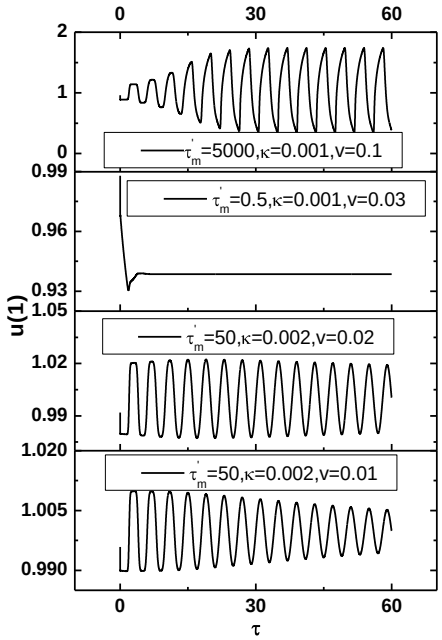

Fig. 2 The simulation of THz generation

We see from Fig. 2 that when τ_m' is very small (the second part, ω_1''=-0.97), even the first mode is rapidly damped out and no oscillation happens, or the oscillation will be gradually damped out, as shown in the fourth part (ω_1''=-0.002). The third part shows that ω_1=0.012 and ω_2=-0.012($\omega_1>\kappa$=0.002), so the first mode is amplified and tends to be stable because of the nonlinear properties. The first part shows the condition that the first 15 modes are all amplified ($\omega_1>>\kappa$), indicating the case of shock wave.

The voltage distribution of the shock wave in the first part of Fig. 2 is shown in Fig. 3. Indices 1 to 10 denote the time points from the dimensionless time 31 to 31.9, with the step of 0.1. The step-like distribution moves from the drain to the source and seldom changes its shape, which is the typical feature of shock waves.

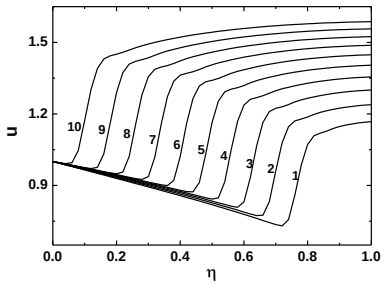

Fig. 3 The voltage distribution of the shock wave

We conclude from the simulation and theory that the higher modes ω_n are amplified if ω_n''>0, but is exponentially small than the first one [2]. The higher modes tend to damp the amplitude. Comparing the first and the third figure in Fig. 2, we conclude that if more modes are amplified, the nonlinear features are clearer because of the existence of the high modes, which coincide with the prediction of the theory, proving the validity of this method.

We notice in Fig. 2 that in a 20 time interval, there are approximately five periods of oscillation, indicating the period T=4. The first dimensionless mode is $\omega=\pi/2$ according to equation (10), and that $\omega T=2\pi$ demonstrates that the theory predicts a sufficiently accurate frequency which also proves the validity of the simulation method. When U_0=3V, L=0.05μm, it is easy to calculate that f=3.63THz.

IV. Simulation of THz Resonant Detection

Using small signal approximation, Dyakonov and Shur have confirmed that the 2DEG in the channel will display resonant response to the incoming signal from the source contact which has the form $U=U_0+U_a\cos\omega t$. Here $U_a<<U_0$ and U_0 is time-independent. The response gate-to-channel voltage U and electron velocity V has the form below and U_i, V_i (i=1, 2, …) is time-dependent:

$$U=\overline{U}+U_1+U_2+... \qquad V=\overline{V}+V_1+V_2+...$$

Compared with the temporal-average of the signal, it is more difficult to measure the amplitude because of the high frequency. The average voltage $\Delta U=\langle U_d\rangle - U_0$ has the relationship with U_0 as below [4], and < > indicates the temporal average in one period:

$$\frac{\Delta U}{U_0}=\frac{1}{4}\left(\frac{U_a}{U_0}\right)^2 f(\omega) \qquad (12)$$

$$f(\omega)=\frac{3\sinh^2(L/2s\tau_m)+\sin^2(\omega L/s)}{\sinh^2(L/2s\tau_m)+\cos^2(\omega L/s)} \qquad (13)$$

$f(\omega)$ is valid when $\omega\tau_m>>1$. According to the numerical method, $\omega L/s=\Omega$, $\tau_m'=\tau_m s/L$, we conclude that the average dimensionless voltage $\Delta u=\Delta U/U_0$ will show peaks at $\Omega=\pi/2$ and its odd harmonics which are the THz wave frequencies of the FET. When τ_m' is sufficiently large, $\sinh(1/2\tau_m')\approx 1/2\tau_m'$, $f(\Omega)\approx 4(\tau_m')^2$ at the peaks. Fig. 4 shows the stable average dimensionless drain voltage under the condition that u_0=1, u_a=0.02, τ_m'=50 and $\Omega=\pi f/2$, and initial conditions are u=1, v=0, with the same physical meaning as that in Section III:

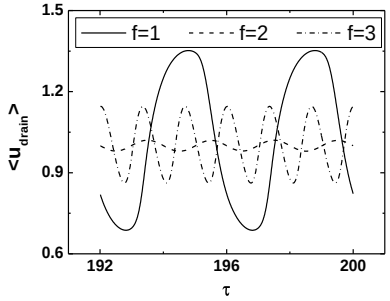

Fig. 4 The stable THz radiation at the drain contact

It is clear that at $\Omega=\pi(2N+1)/2$, the amplitudes are larger than that at the even harmonic which is typical resonant feature, but Fig. 4 does not directly describe Δu. Moreover, the influence of τ_m' to the peaks is needed to be verified, which are shown in Fig. 5.

In Fig. 5, the first part is set at τ_m'=50 and the second one at f=1. Yet the simulation result is a little different from theoretical anticipation. It is the same that the peaks exist at f=(2N+1), but the magnitude is much smaller (0.05 to 1), and neither peak is as sharp as that the theory predicts. At other frequencies result fits well with the theory. Moreover, the second figure does not indicate that $f(\omega)=4(\tau_m')^2$ either. At last, we find from both figures that the resonant frequencies are not accurately f=1 and f=3, but a little smaller than these frequencies.

If $\omega\tau_m<<1$, $f(\omega)$ is reduced to another form [4]:

$$f(\omega)=\frac{\sinh^2\lambda-\sin^2\lambda}{\sinh^2\lambda+\cos^2\lambda} \qquad (14)$$

Here $\lambda=(\Omega/2\tau_m')^{1/2}$, if $\tau_m'<<1$, $\lambda>>1$, $f(\omega)\approx 1$. In this case, the responsivity is much smaller and almost frequency-independent because of the sufficiently strong scattering. The simulation result is as Fig. 6:

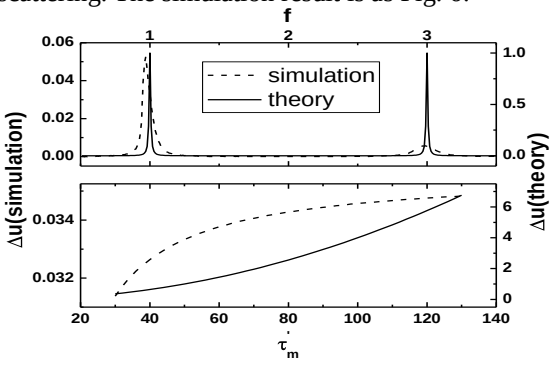

Fig. 5 The influence of f and τ_m' in THz detection

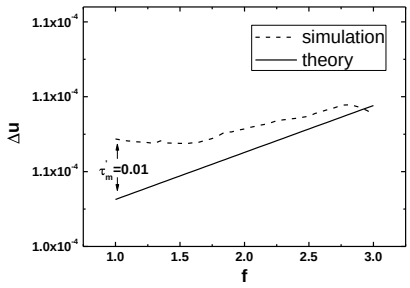

Fig. 6 Responsivity at $\omega\tau_m<<1$

In the simulation, τ_m' is changed into 0.01 and other values keep unchanged. According to equations (12) and (14), we calculate that the frequency-independent voltage $\Delta u \approx 1\times10^{-4}$. As shown in Fig. 6, the simulation result is almost the same as theory anticipation.

To explain the differences, we notice that equation (12) is obtained by assuming that $<U>-U_0$ is of the second order of the small signal U_a. This condition is satisfied in theoretical prediction except at the peaks when $\omega\tau_m>>1$. The theory neglects higher modes of oscillation except the first one, but the curve of f=1 in Fig. 3 shows that the radiation does not have only the fundamental mode when resonance happens. In Section III we have concluded that the nonlinear features are caused by the high modes, and tend to damp out the oscillation. Hence, that the resonant detection theory is not valid when Δu is large enough is proved again by the numerical simulation.

V. Discussion

We find from the simulation that the high modes of radiation cannot be neglected. In THz generation, the high modes tend to damp the amplitude, but do not change the frequency. In THz detection, the frequency responsivity exhibits much lower peaks at the high modes than at the first, and the fundamental mode is dominant in the detection, which provides possibility of accurate measurement of frequency at THz range, due to that the highest peak is related to only ONE frequency. More structures and effects have been considered for THz generation and detection, such as FET with split-gates [8], ungated 2DEG [9], transit-time effects [10], non-ideal side contacts [11], Nanowire MOSFET [12, 13]. The simulation method is also able to provide strong support to the theories mentioned in this issue just by adding different boundary and initial condition.

VI. Conclusion

In this paper a new numerical method for THz FET is developed and discussed. The simulation results coincide with the anticipation of the developed THz theories, and display the predicted defect of the theory of resonant detection, providing physically reasonable results.

Acknowledgement

This work is supported by the National natural Science Funds of China (60976066), the Key Project of National Natural Science Funds of China (601036004), the Shenzhen Science & Technology Foundation (CXB201005250031A), the Fundamental Research Project of Shenzhen Science & Technology Foundation (JC201005280670A), the International Collaboration Project of Shenzhen Science & Technology Foundation （ZYA2010006030006A）.

References

[1] S. J. Allen, Jr., D. C. Tsui and R. A Logan, Phys. Rev. Lett., vol. 38, p. 980 (1977)
[2] A.P. Dmitriev, A. S. Furman and V. Yu. Kachorovskii, Phys. Rev. B, vol. 54, No. 19 (1996)
[3] V. Ryzhii, I. Khmyrova and A. Satou, Journal of Applied Physics, vol. 92, No. 10 (2002)
[4] M. Dyakonov and M. Shur, IEEE TED, vol. 43, No. 3 (1996)
[5] W. Knap, V. Kachorovskii and Y. Deng, Journal of Applied Physics, vol. 91, No. 11 (2002)
[6] M. Dyakonov and M. Shur, Phys. Rev. Lett., vol. 71, No. 15 (1993)
[7] A.P Dmitriev, A. S. Furman and V. Yu. Kachorovskii, Phys. Rev. B, vol. 55, No. 16 (1997)
[8] V. Ryzhii and A. Satou, Journal of Applied Physics, 103, 014504 (2008)
[9] M. Dyakonov and M. Shur, Applied Physics Letters, 87, 111501 (2005)
[10] A. Satou, I Khmyrova and V Ryzhii, Semicond. Sci, Technol. 18, 460-469 (2003)
[11] A. Satou, V. Ryzhii and A. Chaplik, Journal of Applied Physics, 98, 034502 (2005)
[12] J. He, F. Liu and J. Zhang, IEEE TED, vol. 54 No. 5, (2007)
[13] Y. Chen, J. He and X. Mou, etc., Journal of Computational and Theoretical Nanoscience, vol.6, no.10, 2009, pp.2247-2254.